Anal. Chem. **2007,** *79,* 8090−8097

Method for Profiling Mucin Oligosaccharides from Gastric Biopsies of Rhesus Monkeys with and without *Helicobacter pylori* Infection

Cara L. Cooke, Hyun Joo An, Jaehan Kim, Jay V. Solnick, and Carlito B. Lebrilla*

Departments of Internal Medicine and Medical Microbiology & Immunology, Center for Comparative Medicine, Department of Chemistry, Department of Viticulture and Enology, University of California, Davis, California 95616

A method for in vivo analysis of gastric mucin oligosaccharides was developed and applied to rhesus monkeys with and without *Helicobacter pylori* infection. Mucin-type O-linked oligosaccharides were directly released by reductive β-elimination from gastric biopsies from rhesus monkeys. The released oligosaccharides were structurally characterized by matrix-assisted laser desorption/ionozation and electrospray ionization Fourier transform ion cyclotron resonance mass spectrometry. A diverse profile of neutral and acidic oligosaccharides was observed with these techniques. The most predominant core structure detected in all of the samples at relatively high abundance corresponded to core 2 (2HexNAc−1Hex, *m/z* = 611.227). The spectra generated from *H. pylori*-infected monkey samples showed fewer oligosaccharides collectively. Peaks corresponding to 1HexNAc−1Hex (*m/z* = 408.148) and 2HexNAc (*m/z* = 449.174), which most likely represent core structures, were absent in all infected monkeys studied, although present in all uninfected monkeys. Unsupervised cluster analysis demonstrated clear differences between the peaks detected in uninfected and naturally infected monkey samples. The results suggest that *H. pylori* infection is associated with lower relative abundance of oligosaccharides and loss of mucin-type core structures. This method can be applied to characterize the glycans associated with the mucin lining of live animals and allows for repeated analysis of the same animal over the course of infection.

Mucins are large glycoproteins that carry dense clusters of O-linked glycans at serine and threonine residues. Cross-linkage of mucin glycoproteins results in formation of the viscous mucus layer that covers the epithelial surface[1] and is involved in a variety of biological processes, such as attenuation of shear forces, protection against acid, and maintenance of epithelial homeostasis.[2,3] Mucins also serve to protect against commensal and pathogenic bacteria by inhibition of epithelial cell contact and perhaps by forming a bacterial aggregate that can be more easily cleared in peristalsis.[4] On the other hand, bacteria have adapted to exploit glycan moieties that are displayed on mucins for both adherence[5,6] and nutrition.[7] The bacteria−host interaction may in turn result in an alteration of mucin glycosylation patterns that can prevent bacterial binding and recruit inflammatory cells.[8−10] Thus, there is a complex interplay and cross talk between mucins and the bacterial populations that colonize the epithelial surface.

The major bacterial pathogen that colonizes the gastric mucus layer is *Helicobacter pylori*, which in ∼10−15% of those infected results in peptic ulcer disease or gastric cancer.[11] *H. pylori* participates in a variety of interactions with gastric mucins, including adherence to glycan structures,[12] alteration of gastric mucin expression,[13] and modification of glycosylation patterns.[10] One mechanism by which *H. pylori* colonizes the gastric mucosa is through adherence to gastric mucins,[14] including fucosylated ABO blood group antigens[15] and oligosaccharides with charged modifications, such as sialic acid.[16] Binding to fucosylated ABO blood group antigens and sialyl-Le^x (Lewis x) is mediated by the BabA[12] and SabA[16] adhesins, respectively. These proteins are

* To whom correspondence should be addressed. E-mail: cblebrilla@ucdavis.edu. Fax: 1-530-754-5609.

(1) Varki, A.; Cummings, R.; Esko, J.; Freeze, H.; Hart, G.; Marth, J. *Essentials of Glycobiology*, 1st ed.; Cold Spring Harbor Laboratory Press: Cold Spring Harbor, NY, 1999.
(2) Holzer, P. *Curr. Opin. Gastroenterol.* **2000**, *16*, 469−478.
(3) Hang, H. C.; Bertozzi, C. R. *Bioorg. Med. Chem.* **2005**, *13*, 5021−5034.
(4) Hecht, G. *Am. J. Physiol.* **1999**, *277*, C351−358.
(5) Kubiet, M.; Ramphal, R.; Weber, A.; Smith, A. *Infect. Immun.* **2000**, *68*, 3362−3367.
(6) Ramphal, R.; Arora, S. K. *Glycoconjugate J.* **2001**, *18*, 709−713.
(7) Hooper, L. V.; Xu, J.; Falk, P. G.; Midtvedt, T.; Gordon, J. I. *Proc. Natl. Acad. Sci. U.S.A.* **1999**, *96*, 9833−9838.
(8) Lamblin, G.; Degroote, S.; Perini, J. M.; Delmotte, P.; Scharfman, A.; Davril, M.; Lo-Guidice, J. M.; Houdret, N.; Dumur, V.; Klein, A.; Rousse, P. *Glycoconjugate J.* **2001**, *18*, 661−684.
(9) Bry, L.; Falk, P. G.; Midtvedt, T.; Gordon, J. I. *Science* **1996**, *273*, 1380−1383.
(10) Ota, H.; Nakayama, J.; Momose, M.; Hayama, M.; Akamatsu, T.; Katsuyama, T.; Graham, D. Y.; Genta, R. M. *Virchows Arch.* **1998**, *433*, 419−426.
(11) Kusters, J. G.; van Vliet, A. H.; Kuipers, E. J. *Clin. Microbiol. Rev.* **2006**, *19*, 449−490.
(12) Ilver, D.; Arnqvist, A.; Ogren, J.; Frick, I. M.; Kersulyte, D.; Incecik, E. T.; Berg, D. E.; Covacci, A.; Engstrand, L.; Boren, T. *Science* **1998**, *279*, 373−377.
(13) Marques, T.; David, L.; Reis, C.; Nogueira, A. *Pathol. Res. Pract.* **2005**, *201*, 665−672.
(14) Linden, S.; Nordman, H.; Hedenbro, J.; Hurtig, M.; Boren, T.; Carlstedt, I. *Gastroenterology* **2002**, *123*, 1923−1930.
(15) Aspholm-Hurtig, M.; Dailide, G.; Lahmann, M.; Kalia, A.; Ilver, D.; Roche, N.; Vikstrom, S.; Sjostrom, R.; Linden, S.; Backstrom, A.; Lundberg, C.; Arnqvist, A.; Mahdavi, J.; Nilsson, U. J.; Velapatino, B.; Gilman, R. H.; Gerhard, M.; Alarcon, T.; Lopez-Brea, M.; Nakazawa, T.; Fox, J. G.; Correa, P.; Dominguez-Bello, M. G.; Perez-Perez, G. I.; Blaser, M. J.; Normark, S.; Carlstedt, I.; Oscarson, S.; Teneberg, S.; Berg, D. E.; Boren, T. *Science* **2004**, *305*, 519−522.

10.1021/ac071157d CCC: $37.00
Published on Web 10/05/2007

Table 1. Neutral Oligosaccharide Structures Detected in Gastric Antrum from Rhesus Monkeys

		H. pylori uninfected[a]				*H. pylori* infected[a]	
observed mass	oligosaccharide composition	32874	33161	32418	33986	31678	31775
408.148	1HexNAc−1Hex	+	+	+	+	−	−
449.175	2HexNAc	+	+	+	+	−	−
611.227	2HexNAc−1Hex	+	+	+	+	+	+
757.285	2HexNAc−1Hex−1Fuc	+	+	+	+	+	+
773.280	2HexNAc−2Hex	+	+	+	+	+	+
814.307	3HexNAc−1Hex	+	+	+	+	+	+
903.343	2HexNAc−1Hex−2Fuc	+	−	+	−	−	−
919.338	2HexNAc−2Hex−1Fuc	+	+	+	+	+	+
976.360	3HexNAc−2Hex	+	+	+	+	+	+
1122.418	2HexNAc−3Hex−1Fuc	+	+	+	+	+	+
1138.413	3Hex−3HexNAc	+	−	+	+	−	+
1179.439	2Hex−4HexNAc	+	+	+	+	+	+
1268.476	3HexNAc−2Hex−2Fuc	+	+	+	+	+	+
1284.471	3HexNAc−3Hex−1Fuc	+	+	+	+	−	+
1341.492	3Hex−4HexNAc	+	−	+	+	−	−
1373.507	2HexNAc−3Hex−3Fuc	−	+	+	−	−	−
1430.528	3HexNAc−3Hex−2Fuc	+	+	+	+	−	+
1487.550	4HexNAc−3Hex−1Fuc	+	−	+	+	−	−
1503.545	4Hex−4HexNAc	−	+	+	−	−	−
1544.571	3Hex−5HexNAc	−	−	+	−	−	−
1633.610	4HexNAc−3Hex−2Fuc	+	+	−	+	−	−
1649.603	4HexNAc−4Hex−1Fuc	+	−	+	+	−	−

[a] Five-digit numbers refer to animal number.

members of a large family of highly related outer membrane proteins, some of which probably also serve as adhesins to engage in a broad range of interactions with host receptors.[17]

The rhesus macaque provides a physiologically relevant animal model of human *H. pylori* infection that we[18−20] and others[21−23] have used to better understand the *H. pylori*−host interaction. Socially housed rhesus macaques are naturally infected with *H. pylori* that is indistinguishable from that which infects humans.[19,21,23] Derivation of specific-pathogen (*H. pylori*)-free macaques by isolating them at birth provides a ready source of uninfected animals that can be used for experimental *H. pylori* challenge.[18] Infection is characterized by chronic gastritis with infiltration of polymorphonuclear leukocytes, which mimics the gastritis that is a hallmark of *H. pylori* infection in humans. Some infected monkeys develop atrophic gastritis, the histological precursor to gastric adenocarcinoma.[22] Additional similarities that make the rhesus monkey a relevant animal model for investigations of gastric mucins and human disease include expression of human type blood group structures, such as the ABO and Lewis antigens,[24] and receptors for *H. pylori* adhesins, including Le^b, sialyl-Le^x, and sialyl-Le^a.[25]

Since socially housed rhesus monkeys are naturally infected with *H. pylori* that mimics human infection, characterization of the glycan environment of the gastric mucosa of rhesus monkeys may lead to identification of additional host receptors for *H. pylori* adhesins and may further define changes in host glycosylation patterns upon *H. pylori* infection. Here we describe the use of matrix-assisted laser desorption/ionization (MALDI) and electrospray ionization Fourier transform ion cyclotron resonance mass spectrometry (nano-ESI FT-ICR MS) to profile oligosaccharide chains released from gastric biopsies obtained from rhesus monkeys with and without *H. pylori* infection. The results suggest that *H. pylori* infection is associated with lower relative abundance of oligosaccharides and loss of mucin-type core structures. Since the method described in this report is applied to live animals, it allows for repeated analysis of the same animal over the course of infection and will facilitate in-depth in vivo studies of the relationship between gastric mucins and *H. pylori* infection.

EXPERIMENTAL SECTION

Animals and Experimental Design. Seven rhesus macaques between the ages of 5 and 7 years were housed at the California National Primate Research Center (CNPRC), which is accredited by the Association for the Assessment and Accreditation of Laboratory Animal Care. Five monkeys were raised from birth to be free of *H. pylori* and were confirmed to be uninfected according to protocols described previously.[18] One of these five monkeys was studied before and after experimental challenge with *H. pylori*

(16) Mahdavi, J.; Sonden, B.; Hurtig, M.; Olfat, F. O.; Forsberg, L.; Roche, N.; Angstrom, J.; Larsson, T.; Teneberg, S.; Karlsson, K. A.; Altraja, S.; Wadstrom, T.; Kersulyte, D.; Berg, D. E.; Dubois, A.; Petersson, C.; Magnusson, K. E.; Norberg, T.; Lindh, F.; Lundskog, B. B.; Arnqvist, A.; Hammarstrom, L.; Boren, T. *Science* **2002**, *297*, 573−578.

(17) Alm, R. A.; Bina, J.; Andrews, B. M.; Doig, P.; Hancock, R. E.; Trust, T. J. *Infect. Immun.* **2000**, *68*, 4155−4168.

(18) Solnick, J. V.; Canfield, D. R.; Yang, S.; Parsonnet, J. *Lab. Anim. Sci* **1999**, *49*, 197−201.

(19) Solnick, J. V.; Chang, K.; Canfield, D. R.; Parsonnet, J. *J. Clin. Microbiol.* **2003**, *41*, 5511−5516.

(20) Solnick, J. V.; Hansen, L. M.; Canfield, D. R.; Parsonnet, J. *Infect. Immun.* **2001**, *69*, 6887−6892.

(21) Drazek, E. S.; Dubois, A.; Holmes, R. K. *J. Clin. Microbiol.* **1994**, *32*, 1799−1804.

(22) Dubois, A.; Berg, D. E.; Incecik, E. T.; Fiala, N.; Heman-Ackah, L. M.; Perez-Perez, G. I.; Blaser, M. J. *Infect. Immun.* **1996**, *64*, 2885−2891.

(23) Dubois, A.; Fiala, N.; Heman-Ackah, L. M.; Drazek, E. S.; Tarnawski, A.; Fishbein, W. N.; Perez-Perez, G. I.; Blaser, M. J. *Gastroenterology* **1994**, *106*, 1405−1417.

(24) Socha, W. W.; Moor-Jankowski, J.; Ruffie, J. *J. Med. Primatol.* **1984**, *13*, 11−40.

(25) Linden, S.; Boren, T.; Dubois, A.; Carlstedt, I. *Biochem. J.* **2004**, *379*, 765−775.

Table 2. Acidic Oligosaccharide Structures Detected in Gastric Antrum from Rhesus Monkeys

		H. pylori uninfected[a]		*H. pylori* infected[a]
observed mass	oligosaccharide composition	32874	33161	31678
667.187	2HexNAc−1SO_3H−1Hex	−	+	−
675.250	1HexNAc−1NeuAc−1Hex	−	+	−
716.273	2HexNAc−1NeuAc	+	+	+
821.304	1HexNAc−1Fuc−1NeuAc−1Hex	+	+	−
829.240	2HexNAc−1SO_3H−2Hex	+	−	−
878.326	2HexNAc−1NeuAc−1Hex	+	+	−
966.340	1HexNAc−2NeuAc−1Hex	+	+	−
1024.384	2HexNAc−1Fuc−1NeuAc−1Hex	−	+	+
1081.405	3HexNAc−1NeuAc−1Hex	−	−	−
1170.442	2HexNAc−2Fuc−1NeuAc−1Hex	−	+	+
1266.390	2HexNAc−1Fuc−1NeuAc−1SO_3H−2Hex	−	−	+
1315.480	2HexNAc−1Fuc−2NeuAc−1Hex	−	+	+
1697.630	3HexNAc−2Fuc−1NeuAc−3Hex	+	+	−

[a] Five-digit numbers refer to animal number.

strain J166, which preferentially colonizes rhesus macaques.[20] Two monkeys were socially housed and naturally infected with *H. pylori*. Infection was documented by culture of gastric biopsies obtained by endoscopy as previously described.[18] All procedures were approved by the CNPRC Research Advisory Committee and by the University of California, Davis, Chancellor's Animal Use and Care Administrative Advisory Committee.

Release of O-Linked Oligosaccharides from Gastric Biopsies. Three biopsies were obtained from the gastric antrum and corpus of each monkey. Biopsies were placed in 250 μL of 70% ethanol, homogenized with a sterile glass rod, and dialyzed (MW cutoff 12 000−14 000) against 2 L of nanopure H_2O at room temperature for 3 days. The material retained in the dialysis tubing was lyophilized, and 1−3 mg was added to 500 μL of alkaline borohydride solution (mixture of 1.0 M sodium borohydride and 0.1 M sodium hydroxide, Sigma-Aldrich). The mixture was incubated at 42 °C for 12 h in a water bath, and the reaction was stopped by addition of 1.0 M hydrochloric acid solution in an ice bath to destroy excess sodium borohydride.

Oligosaccharide Purification by Porous Graphitized Carbon Solid-Phase Extraction. O-Linked oligosaccharides released by reductive β-elimination were purified by solid-phase extraction using a porous graphitized carbon cartridge (Alltech Associates, Deerfield, IL). The cartridge was washed with H_2O followed by 0.05% (v/v) trifluoroacetic acid in 80% acetonitrile (ACN)/H_2O (v/v). The solution of released oligosaccharide was loaded on the cartridge and washed with Nanopure water at a flow rate of ∼1 mL/min to remove salts and buffer. O-Linked glycans were eluted with 10% ACN in H_2O, 20% ACN in H_2O, and 40% ACN in H_2O with 0.05% trifluoroacetic acid. Each fraction was collected and dried in a Centrivap apparatus. Fractions were reconstituted in Nanopure water prior to MS analysis.

Mass Spectrometric Analysis. Mass spectra were recorded on an external source HiResMALDI (IonSpec Corp., Irvine, CA) equipped with a 7.0-T magnet. The HiResMALDI was equipped with a pulsed Nd:YAG laser (355 nm). 2,5-Dihydroxybenzoic acid and 2,5-dihydroxyacetophenone were used as a matrix (5 mg/100 μL in 50% ACN in H_2O) for positive and negative modes, respectively. A saturated solution of NaCl in 50% ACN in H_2O was used as a cation dopant. The oligosaccharide solution (1 μL) was applied to the MALDI probe followed by matrix solution (1 μL). The sample was dried under a stream of air prior to mass spectrometric analysis.

A HiResESI (IonSpec Corp.) instrument equipped with a 9.4-T magnet and Picoview nano-ESI source (New Objective, Woburn, MA) was used to obtain more sensitive detection of acidic oligosaccharides. Sample solutions for the nanoelectrospray source were delivered using a standard six-port switching valve and an Eksigent 1D pump (Eksigent Technologies, Livermore, CA). Sample solutions were delivered with a flow rate of 250 nL/min composed of 0.1% formic acid in 50/50 water/ACN (v/v).

Unsupervised Cluster Analysis. Unsupervised cluster analysis was performed in order to systematically compare oligosaccharide profiles of *H. pylori* infected (32874, 33161, 32418, and 33986) and uninfected (31678 and 31775) monkeys. Absolute peak intensities from Table 1 were normalized across spectra and clustered using HCE 3.5 software (http://www.cs.umd.edu/hcil/hce). Pearson's r was used to calculate similarity, and each cluster was updated and drawn using the complete linkage method.

RESULTS

A major initial concern in the development of this method was whether sufficient quantities of gastric biopsy material could be obtained to extract enough sample for mass analysis to profile the oligosaccharides in gastric mucins. An additional concern was whether mucins would indeed be obtained in the process. Both concerns were readily addressed by performing mass profiles of the samples and examining the masses for glycan compositions. Accurate mass capabilities often provide unambiguous assignments of glycan peaks, while the composition provides direct evidence for whether mucin oligosaccharides are obtained or N-linked oligosaccharides, which are often indicators for nonmucinous glycoproteins.

Gastric biopsy samples were obtained from both antrum and corpus, but significantly more abundant oligosaccharide signals were detected from the antrum samples. Single biopsies were processed individually, but these samples generated weak signals when analyzed by mass spectrometry. In order to improve the mass spectrometry signal detection, three biopsies from the same animal were pooled prior to sample processing. Subsequent analysis of corpus samples with a more sensitive upgrade of the MS instrument showed that the oligosaccharide signals in the

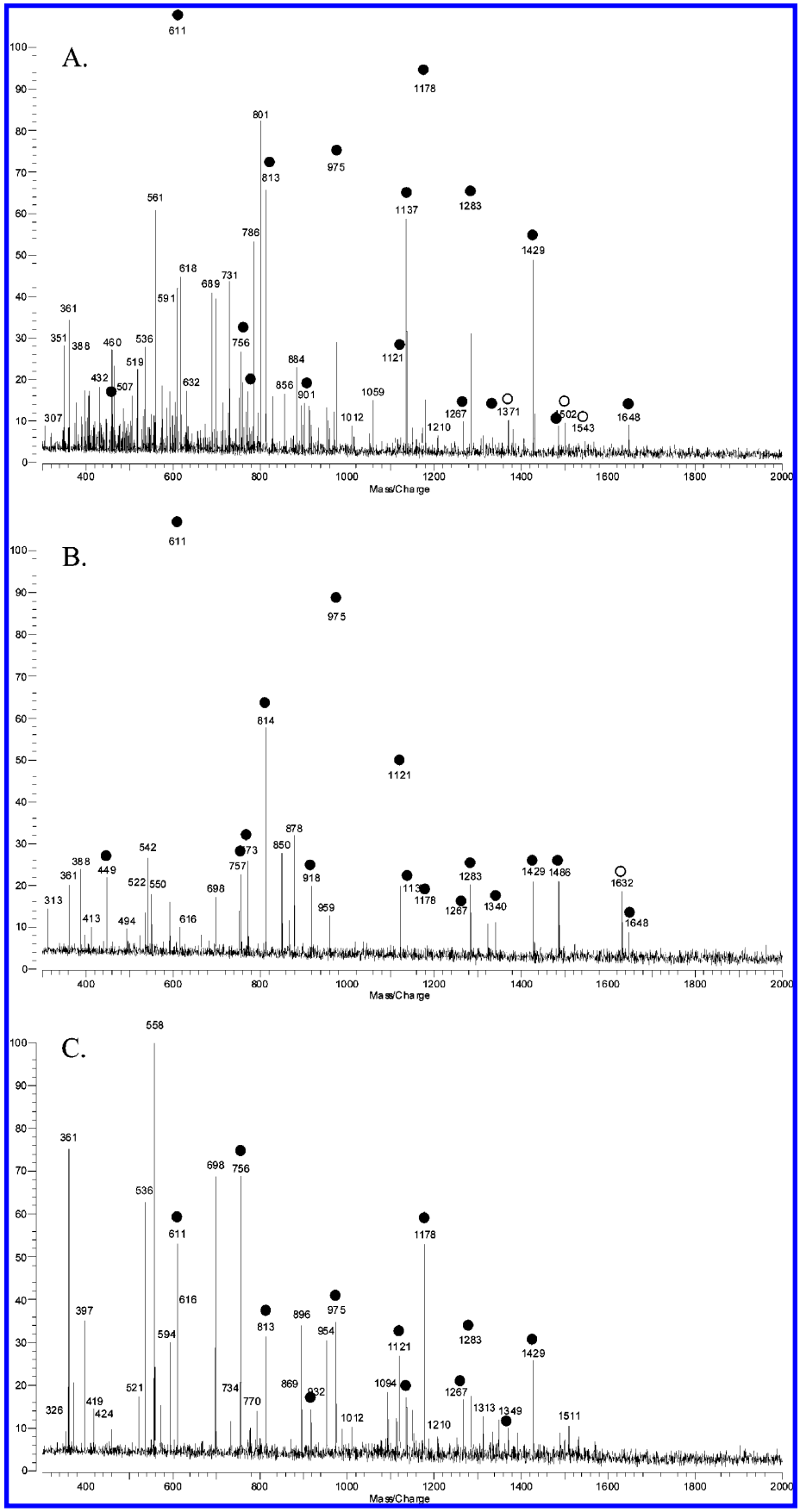

Figure 1. MALDI-FTMS spectra of 10% ACN fraction in positive mode of antral biopsies from (A) a single uninfected monkey, (B) the same uninfected monkey 10 weeks later, and (C) a single naturally infected monkey. ● indicates peaks corresponding to oligosaccharide structures present at both time points. ○ indicates differences in the two spectra taken 10 weeks apart.

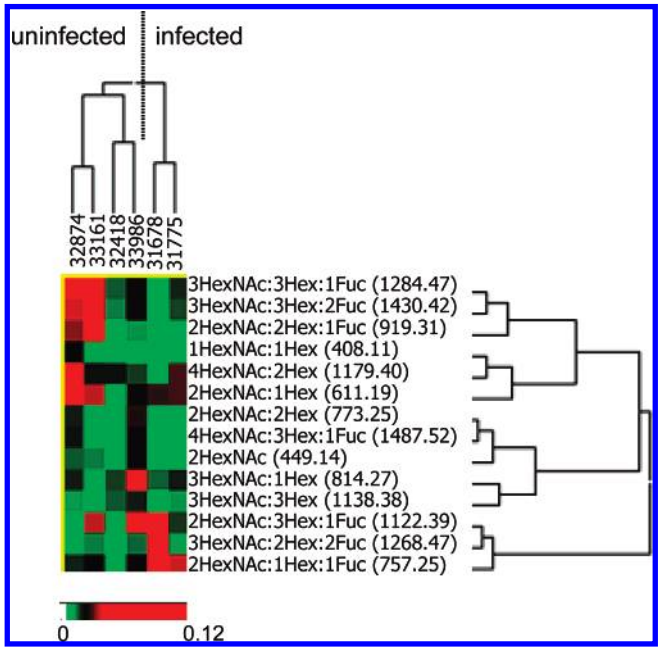

Figure 2. Unsupervised cluster analysis of oligosaccharides identified in gastric mucosa of *H. pylori* infected (32874, 33161, 32418, and 33986) and uninfected (31678 and 31775) monkeys.

corpus were less abundant than those in the antrum (data not shown). Therefore, the antrum samples became the focus of this study.

After removing salts and small molecules with dialysis, the samples were treated with reductive β-elimination to release mucin-type O-linked oligosaccharides present in the pooled biopsies. The resulting samples were purified and fractionated using solid-phase extraction and solvents of varying polarity (10, 20, and 40% ACN in water) to partition them into highly anionic and neutral components. The fractions were then analyzed directly by mass spectrometry in both the positive (cation) and negative (anion) modes. The 40% ACN fractions did not contain detectable glycans. The 10 and 20% fractions generated similar glycan profiles of predominantly small, neutral species (Table 1) and some acidic structures (Table 2) that were all consistent with small O-linked mucin-type oligosaccharides. The masses and specific composition further corresponded to the respective alditol, which are consistent with the specific release procedures employed in the analysis.

In order to examine reproducibility of mass spectra generated from the same monkey over time, we analyzed the MALDI MS spectra generated from biopsies taken from the same uninfected monkey 10 weeks apart (Figure 1A and B). The spectra generated from the antrum samples showed peaks that primarily correspond to oligosaccharide structures and further illustrate that abundant ions are obtained when three biopsy samples are combined. The oligosaccharide profiles generated from these independent biopsies also showed remarkable stability over time, as the only difference between these two spectra was the presence of three structurally related peaks of relatively low abundances (m/z 1373.502, 1503.545, 1544.571) in the earlier biopsy samples and a single peak (m/z 1633.607) also of low abundance in the later biopsy samples. Analysis of samples obtained from the same monkey on the same day that were processed separately indicated that these variations are likely due to the solid-phase extraction and not necessarily to biological changes or to the mass spectrometry.

We next compared the spectra obtained from uninfected monkeys to those obtained from naturally infected monkeys. Panels A and B in Figure 1 show MALDI mass spectra from a single uninfected monkey collected 10 weeks apart (10% fractions). Figure 1C depicts the spectrum generated from one naturally infected monkey. The neutral oligosaccharides observed in all fractions obtained from both uninfected and naturally infected monkeys are listed in Table 1. Oligosaccharide compositions were obtained based on accurate mass analysis (<5 ppm mass accuracy). The compositions confirmed the presence of primarily neutral oligosaccharides comprised of mucin core-type structures containing *N*-acetylhexosamine (HexNAc) and hexose (Hex) residues, either with or without fucosylation. As shown in Table 1, the dominant mass in all of the samples (infected and uninfected), at relatively high abundances, corresponded to core 2 (2HexNAc−1Hex, $m/z = 611.227$). Core 1 and core 2 structures are commonly found in all mammals.[26] Core 2 structures have unique compositions that allow rapid identification in mass spectra. The spectra generated from *H. pylori*-infected monkey samples showed fewer oligosaccharides collectively. Peaks corresponding to 1HexNAc−1Hex (m/z = 408.148) and 2HexNAc (m/z = 449.174), which are most likely core structures 1 and 4, respectively, were absent in all infected monkeys, although present in all uninfected monkeys. In addition, several structures with m/z greater than 1300 were absent in the infected monkeys.

In order to systematically compare oligosaccharide profiles of uninfected and naturally infected monkeys, we performed unsupervised cluster analysis. The absolute peak intensities from Table 1 were normalized across spectra and clustered using HCE 3.5 software (http://www.cs.umd.edu/hcil/hce). Pearson's r was used to calculate similarity, and each cluster was updated and drawn using the complete-linkage method. The dendrogram in Figure 2 demonstrates clear differences between the oligosaccharide peaks detected in uninfected and naturally infected monkey samples.

Additional samples from uninfected and naturally infected animals were then analyzed using nano-ESI MS, which for this study showed greater sensitivity than MALDI MS and provided enhanced detection of acidic oligosaccharides, particularly in the negative mode. Nano-ESI was used to confirm the MALDI results, though, due to sample limitations, not all samples were examined with both ionization methods. The nano-ESI spectra acquired in the positive mode corroborated the spectra obtained by MALDI-MS. The peaks observed in MALDI (Figure 1A,B) corresponded well to those obtained by ESI (Figure 3A), as a similar distribution of peaks was observed with both methods. Nano-ESI spectra acquired in the negative ion mode were examined in an uninfected monkey (Figure 3C) and a naturally infected monkey (Figure 3D). Sialylated and sulfated oligosaccharide species were clearly detected in the nano-ESI spectra (Table 2). The nano-ESI spectra also corroborated the MALDI MS spectra in showing fewer oligosaccharides in the *H. pylori*-infected monkeys compared to the uninfected group. In accordance with the MALDI experiments, the oligosaccharides of higher mass were absent in the infected monkeys (Figure 3A and B).

(26) Van den Steen, P.; Rudd, P. M.; Dwek, R. A.; Opdenakker, G. *Crit. Rev. Biochem. Mol. Biol.* **1998**, *33*, 151−208.

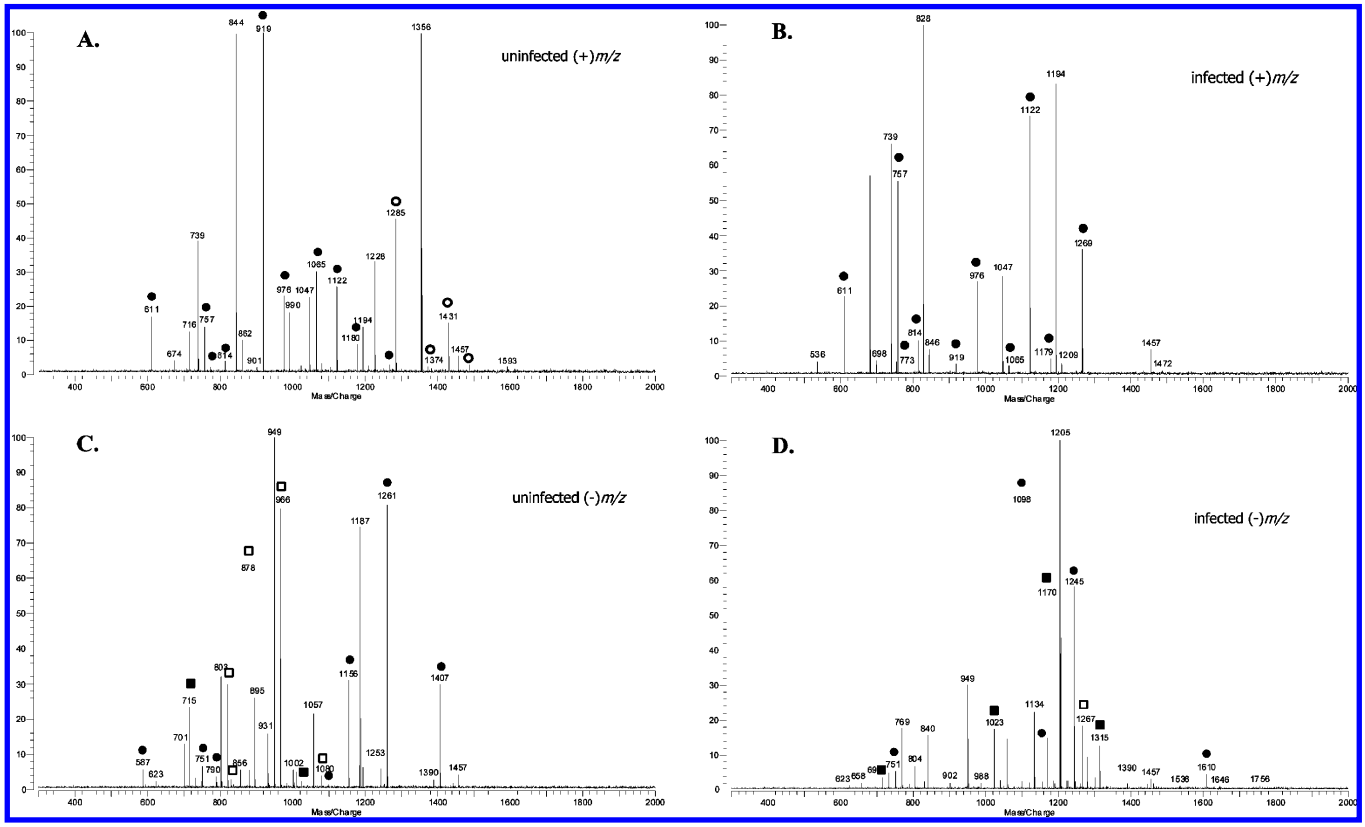

Figure 3. Nano-ESI spectra generated from (A) the 20% ACN fraction obtained from an uninfected monkey acquired in the positive ion mode, (B) the 20% ACN fraction obtained from an infected monkey acquired in the positive ion mode, (C) the 20% ACN fraction obtained from a naturally uninfected monkey acquired in the negative ion mode, and (D) the 20% ACN fraction obtained from a naturally infected monkey acquired in the negative ion mode. ● and ■ indicate neutral and acidic oligosaccharides, respectively, common to spectra from infected and uninfected monkeys. ○ and □ indicate neutral and acidic oligosaccharides, respectively, unique to spectra from infected and uninfected monkeys. All signals correspond to deprotonated molecular ion form ($[M - H]^-$). ● indicates neutral oligosaccharides. ■ represents acidic oligosaccharides.

In order to study glycosylation changes that occur after experimental challenge with *H. pylori*, we analyzed biopsies obtained from a monkey before and 8 months after challenge with *H. pylori* strain J166. The mass spectra generated from the *H. pylori*-challenged monkey acquired in the positive and negative modes are shown in Figure 4A and B, respectively. Table 3 summarizes the neutral oligosaccharides observed at the two time points. Several low molecular weight oligosaccharides were absent postchallenge that were detected in a single biopsy taken from this monkey prechallenge, including peaks corresponding to 1HexNAc−1Hex ($m/z = 408.148$) and 2HexNAc ($m/z = 449.174$). This observation is similar to the finding in the naturally infected monkeys (Table 1). However, there are variations between the *H. pylori*-challenged monkey and the naturally infected monkeys with respect to the higher molecular weight oligosaccharides, which were detected in both the *H. pylori*-challenged and uninfected monkeys, but not in the naturally infected monkeys.

CONCLUSIONS

In this study, we have shown that mass spectrometry can be used to profile mucin oligosaccharides released directly from biopsy tissue without purification of mucin glycoproteins. This allows for rapid profiling of individual structures from a mixed mucin oligosaccharide population with minimal sample preparation. The results suggest that *H. pylori* infection is associated with fewer oligosaccharides and the loss of specific core-type structures.

Mass spectrometry has emerged as the premier technique for the analysis of glycan moieties from biologically important molecules.[27−29] Mass spectrometry offers distinct advantages over conventional approaches because of its inherent sensitivity and speed. The instrument used for this study was a FT-ICR mass spectrometer with both MALDI and nano-ESI ionization sources. This instrument is well-known for high mass accuracy (<5 ppm with external calibration) and high resolution (>100 000 full width at half-height). This means that oligosaccharides are readily identified solely based on their mass. The exact composition with regard to hexoses, *N*-acetylhexosamines, sialic acids, and fucoses are now known and determined from the accurate masses. For example, an oligosaccharide with quasimolecular ion at m/z 1649.602 has three possible compositions within a tolerance of ±0.1 mass unit. Only with a tolerance of 0.01 mass unit is the correct composition of one fucose (Fuc), four Hex, and four HexNAc obtained.

Robbe et al. used nano-ESI quadropole time-of-flight tandem MS to describe the structural diversity of O-linked glycans

(27) An, H. J.; Ninonuevo, M.; Aguilan, J.; Liu, H.; Lebrilla, C. B.; Alvarenga, L. S.; Mannis, M. J. *J. Proteome Res.* **2005**, *4*, 1981−1987.
(28) An, H. J.; Miyamoto, S.; Lancaster, K. S.; Kirmiz, C.; Li, B.; Lam, K. S.; Leiserowitz, G. S.; Lebrilla, C. B. *J. Proteome Res.* **2006**, *5*, 1626−1635.
(29) An, H. J.; Lurie, S.; Greve, L. C.; Rosenquist, D.; Kirmiz, C.; Labavitch, J. M.; Lebrilla, C. B. *Anal. Biochem.* **2005**, *338*, 71−82.

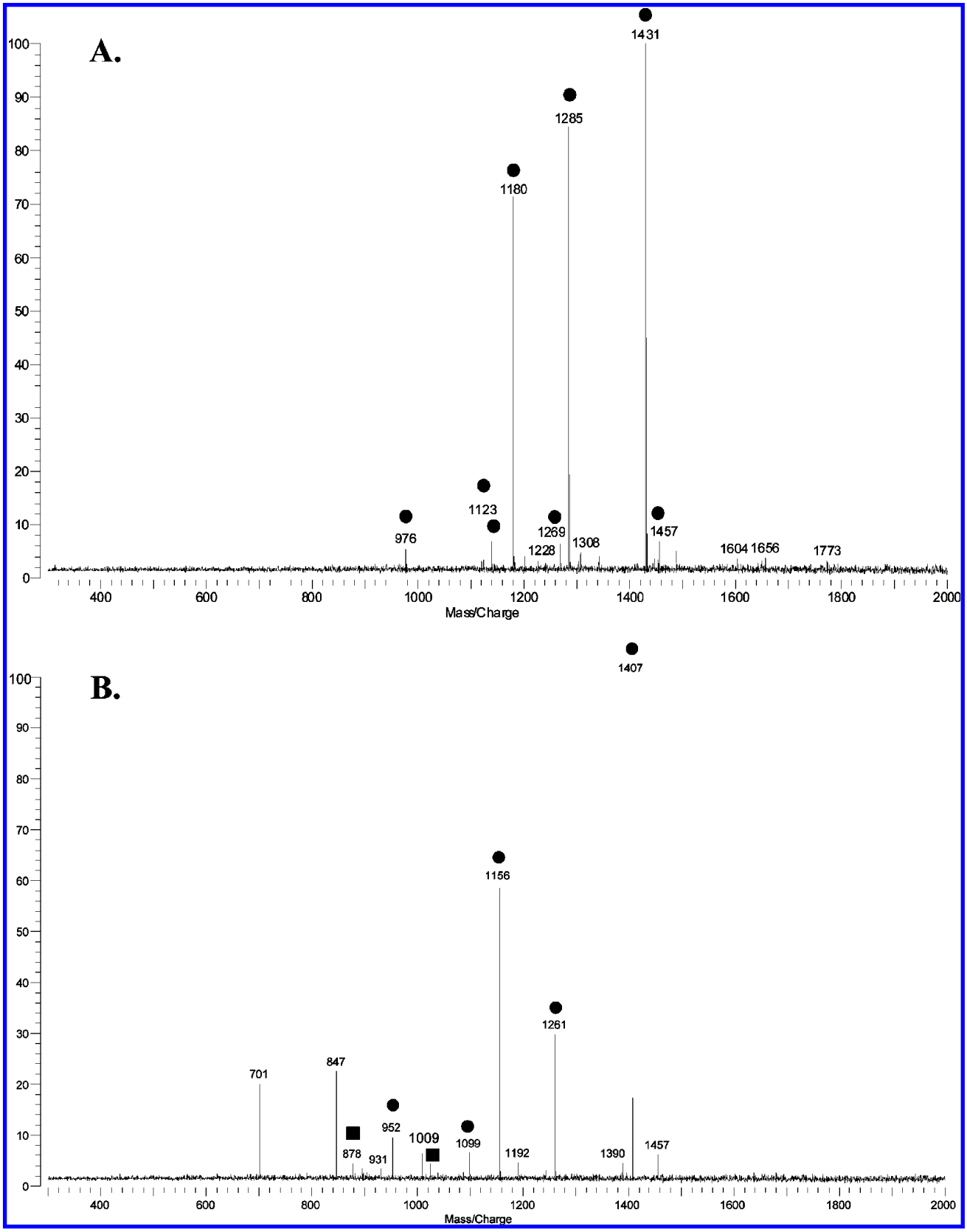

Figure 4. Nano-ESI spectra of the 10% ACN fractions obtained from antral biopsies taken from a single monkey postchallenge in (A) positive mode and (B) negative mode.

released from human mucins from different parts of the intestinal tract.[30] Interestingly, we detected many of the same oligosaccharide structures in gastric mucins of rhesus macaques, including the same core structures and lower molecular weight neutral and acidic structures. However, the stomach of the rhesus macaque appears to display a broader array of larger molecular weight neutral oligosaccharides. Additionally, the predominant core structure detected in the rhesus stomach was core 2.

Table 3. Neutral Oligosaccharide Structures Detected in Gastric Antrum Obtained from a Rhesus Macaque Pre- and Postchallenge with *H. pylori* Strain J166

observed mass	oligosaccharide composition	*H. pylori* uninfected[a]	*H. pylori* inoculated[b]
408.1481	HexNAc−1Hex	+	−
449.175	2HexNAc	+	−
611.227	2HexNAc−1Hex	+	−
757.285	2HexNAc−1Hex−1Fuc	+	−
773.280	2HexNAc−2Hex	+	−
814.307	3HexNAc−1Hex	+	−
903.344	2HexNAc−1Hex−2Fuc	−	−
919.338	2HexNAc−2Hex−1Fuc	+	−
976.360	3HexNAc−2Hex	+	+
1122.418	2HexNAc−3Hex−1Fuc	+	+
1138.413	3Hex−3HexNAc	+	+
1179.440	2Hex−4HexNAc	+	+
1268.476	3HexNAc−2Hex−2Fuc	−	+
1284.471	3HexNAc−3Hex−1Fuc	+	+
1430.528	3HexNAc−3Hex−2Fuc	+	+
1487.550	4HexNAc−3Hex−1Fuc	−	+

[a] Results of a single biopsy. [b] Results of 3 combined biopsies 8 months postchallenge.

It has been postulated that one important pathogenic property of *H. pylori* is its ability to weaken the mucous gel that protects the gastric epithelium.[31] *H. pylori* infection has been found to inhibit total mucin synthesis in gastric epithelial cell lines and was also found to decrease expression of the MUC5AC and MUC1 mucins.[31] Our observations of overall decreased levels of oligosaccharides in *H. pylori* infected monkeys are consistent with decreased expression of mucin glycoproteins.

The absence of peaks corresponding to 1HexNAc−1Hex (m/z = 408.148) and 2HexNAc (m/z = 449.174) in *H. pylori*-infected monkeys is intriguing. 1HexNAc−1Hex most likely represents the core 1 structure. 2HexNAc most likely represents core 3, since this core structure is most common in the intestinal tract.[30] These structures were also undetected in samples obtained from the monkey challenged with *H. pylori* strain J166, although they were detected in the prechallenge samples. The *H. pylori*-challenged monkey also lost many oligosaccharides in addition to the core structures. It is possible that this is an early response to *H. pylori* infection, which differs from that seen in the naturally infected animals that have likely been colonized for several years. Alternatively, differences in oligosaccharides between experimentally and naturally infected monkeys may be a strain-specific effect, since the challenge strain J166 is not identical to strains native to the rhesus monkey.

The procedure described provides a number of potential applications that can be utilized to study the effect of infection on mucin glycans in animal model systems and even humans. The method is relatively noninvasive and can be performed repeatedly on the same subject, thus allowing for time course studies of mucin glycans over the course of infection. The application of this method to the rhesus macaque model of *H. pylori* infection provides an ideal system for examining mucin glycosylation changes that occur during initial infection and over the course of disease development over time.

(30) Robbe, C.; Capon, C.; Coddeville, B.; Michalski, J. C. *Biochem. J.* **2004**, *384*, 307−316.
(31) Byrd, J. C.; Yunker, C. K.; Xu, Q. S.; Sternberg, L. R.; Bresalier, R. S. *Gastroenterology* **2000**, *118*, 1072−1079.

ACKNOWLEDGMENT

This work was supported in part by Public Health Service Grant AI42081 and GM 490077 from the National Institutes of Health. C.L.C. was supported by Training Grant T32 AI060555 from the National Institutes of Health.

Received for review June 1, 2007. Accepted August 13, 2007.

AC071157D